Jurnal Teknologi

Full Paper

NUMERICAL COMPUTATION OF LIGAND AND SIGNAL ASSOCIATED TO INVADOPODIA FORMATION

Noorehan Yaacob[a*], Sharidan Shafie[a], Takashi Suzuki[b], Mohd Ariff Admon[a]

[a]Department of Mathematical Sciences, Faculty of Science, Universiti Teknologi Malaysia, 81310 UTM Johor Bahru, Johor, Malaysia
[b]Division of Mathematical Science, Osaka University, Osaka, Japan

Article history
Received
29 October 2021
Received in revised form
28 February 2022
Accepted
18 March 2022
Published Online
20 June 2022

*Corresponding author
noorehan3@graduate.utm.my

Graphical abstract

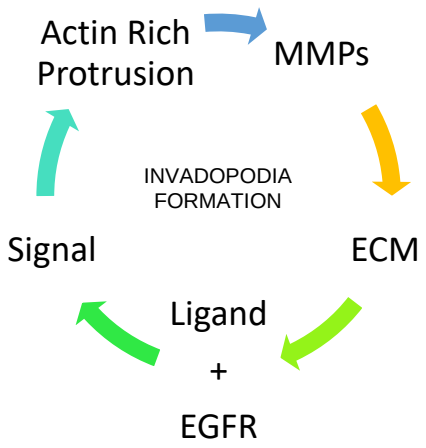

Abstract

Invadopodia are protrusions that are commonly spotted at the plasma membrane of the invasive cancer cells. In forming invadopodia, several molecular interactions are involved such as the ligand, extracellular matrix (ECM), matrix metalloproteinases (MMPs), actin, and signal which are interrelated. In this paper, the mathematical model of ligand and signal transduction is taken in the heat equation with the MMPs is set as function g. Besides, the actin regulation moved the interface and thus computed as the signal gradient. The mathematical model is solved using the combination of methods finite difference, ghost fluid with linear extrapolation, and level set. Apart from that, the convergence results are also given to determine the effectiveness of the above-mentioned methods. Results showed that the stimulation of signal transduction from the ligand and membrane-associated receptor binding consequently moved the plasma membrane. Also, the methods used gave a good agreement in the convergence results.

Keywords: Finite difference, free boundary, ghost fluid, level set, invasive cancer cell

Abstrak

Invadopodia adalah penonjolan yang dilihat pada membran plasma sel kanser invasif. Dalam membentuk invadopodia, beberapa interaksi molekul terlibat seperti ligan, matriks ekstraselular (ECM), matriks metalloproteinase (MMPs), aktin, dan isyarat yang saling berkaitan. Dalam makalah ini, model matematik ligan dan transduksi isyarat diambil dalam persamaan seperti haba dengan MMP ditetapkan sebagai fungsi g. Selain itu, aktin menggerakkan antara muka dan dikira sebagai kecerunan isyarat. Model matematik diselesaikan menggunakan gabungan kaedah perbezaan terhingga, bendalir jelmaan dengan ekstrapolasi linear, dan set aras. Selain itu, keputusan penumpuan juga diberikan untuk menentukan keberkesanan kaedah yang dinyatakan di atas. Keputusan menunjukkan bahawa rangsangan transduksi isyarat daripada ligan dan pengikatan reseptor berkaitan membran seterusnya menggerakkan membran plasma. Juga, kaedah yang digunakan memberikan persetujuan yang baik dari segi hasil penumpuan.

Kata kunci: Perbezaan terhingga, sempadan bebas, bendalir jelmaan, set tahap, sel kanser invasif

1.0 INTRODUCTION

As mentioned by [1], [2], the invadopodia are protrusions that have the ability to open the pathway for the motility of the cancer cells. These structures are involved directly in the metastasis and consequently, invasion of cancer occurred. The molecular interactions including the polymerization of actin, degradation of ECM by the MMPs, creation of ligand, signaling process through membrane receptor, and delivery of MMPs to the invasion front are the processes for the invadopodia formation. According to [3], the force from the polymerization of actin and matrix degradation chemical activity are the causes for the invadopodia to gain their protrusive structure. The MMPs played the role of the matrix-degrading enzymes (MDEs) to degrade the ECM. Meanwhile, the polymerization of actin produced the force that pushed the membrane to enable the growth of the invadopodium.

Studies on invadopodia has been investigated by many researchers due to its important role in the metastasis process [4]–[7]. In an effort to investigate the formation and maturation of invadopodia from a mathematical point of view, [8] introduced a positive feedback loop to explain the process of invadopodia formation. On that account, the mathematical modeling approach has been explained by emphasizing the equations for ECM, MMPs, ligand, and actin. The different rate constants for MMPs are marked to study the level of invasiveness of a cancer cell. This study revealed that the higher of rate constant for MMP, the cancer cell became more invasive. However, the problem appeared as the region of actin became disconnected. Due to the obstacle, actin is noticed at the outside of the cancer cell, and this is not in line with biological facts that actin must lie inside the cancer cell.

To solve the actin disconnection problem, [9], [10] implemented a new domain of a free boundary interface to separate the activities on the regions of inner and outer of the cell. Also, a new variable is suggested which is signal transduction that lies inside the cell. From the numerical results, it is found that, as time increased, the position of the free boundary and density of signal distributions are increased. In addition, the concentration of the signal is spotted higher on the interface. From this attempt, the invadopodium should be formed due to the expansion of the plasma membrane.

Another exploration on the invadopodia that emphasized signal transduction has been performed by [11]. Two-dimensional signal transduction is carried out and from this approach, the invadopodia through the formation of outward protrusions have been disclosed. Besides, [12] also studied the formation of the protrusions by implementing ligand and signal transduction in their mathematical model. In their study, the cell protrusion is accounted as the free boundary by emphasizing the quasi-static mathematical model with the Dirichlet and Neumann condition applied to the inner and outer of the cell, respectively. Further, [13] has studied the two-dimensional time-independent signal and ligand with the Dirichlet boundary condition for both regions.

Generally, the changes of the interface position from the polymerization activity led to the appearance of invadopodia. Hence, it is precise to account for the interface as a free boundary. Thus, the level set is an appropriate method to locate the interface location. Furthermore, the regions of the inner and outer of the cell can be determined using the method of level set.

As mentioned in [14], [15], the level set method is reasonable especially for the boundaries and interfaces tracking in the progression of time. An investigation on the level set method to locate the moving fronts in multi-physics problems is presented by [16]. The techniques of the level set to several problems are stated in [17]. Besides, the method of level set to highlight the changes of interface for the pure substance such as melting of ice or called Stefan problem have been implemented by [18].

Studies in [19]–[21] employed the method of level set to model the growth and interaction of multiple dendrites in solidification. Apart from that, [22], [23] investigated the corrosion effect on the geometry of metals with the implementation of the level set method. Meanwhile, the implementation of the method of level set in a sense of biology has been discussed in [24] to determine the development of cell growth. Thus, from the previous studies, the level set method is appropriate to deal with the interface changes.

Hence, by considering the above-mentioned studies, the formation of invadopodia is investigated by considering the mathematical model of time-dependent ligand and signal transduction. The location of the interface is captured with the zero-level set function approach. Besides, the equations for ligand and signal transduction are solved numerically using finite difference methods. Apart from that, the convergence results are given to explain the effectiveness of the numerical computation.

2.0 METHODOLOGY

2.1 Mathematical Modeling

In this section, four key variables are focused on in this paper to interpret the molecular interactions between ligand denoted by c^*, signal denoted by σ, the interface velocity denoted by v, and velocity extension denoted by w. The molecular interactions between the variables are described in the square domain as pictured in Figure 1 and are defined in $\Omega = 0_t^{c^*} \cup \Gamma_t \cup 0_t^{\sigma}$ to represent the extracellular, interface, and intracellular regions, respectively.

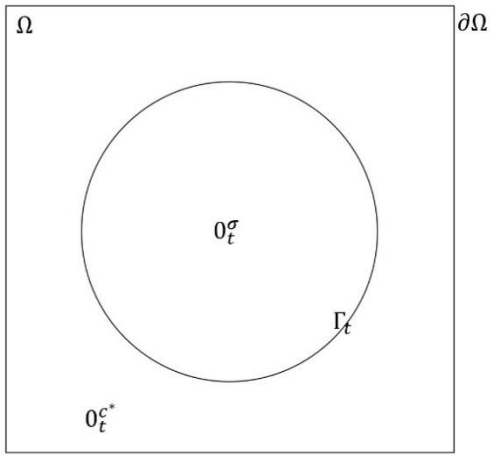

Figure 1 Two-dimensional setting

Meanwhile, Figure 2 portrayed the schematic diagram for the biological process of invadopodia formation. The schematic diagram indicates the ligands are created with the occurrence of ECM degradation by the MMPs and thus ligand diffused to the extracellular region. In this study, the ligands are not accumulated at the square domain. Besides, the flux of MMPs is concentrated on the interface. Hence, the ligand on the interface is set as a function g where $g(\boldsymbol{x}) = \epsilon[2 + \cos(3\pi(x+y))\cos(\pi(x+0.3))]$, [12] and $\epsilon = 10^{-3}$. The ligand binds with the membrane-associate receptor particularly the epidermal growth factor receptor (EGFR) and stimulates the signal transduction. One of the processes that are pivotal for the formation of invadopodia is signal and this is not mentioned in [8]. However, it is introduced in [9], [10], [12]. Therefore, the stimulation of the signal transduction in the intracellular region leads to the MMPs up-regulation.

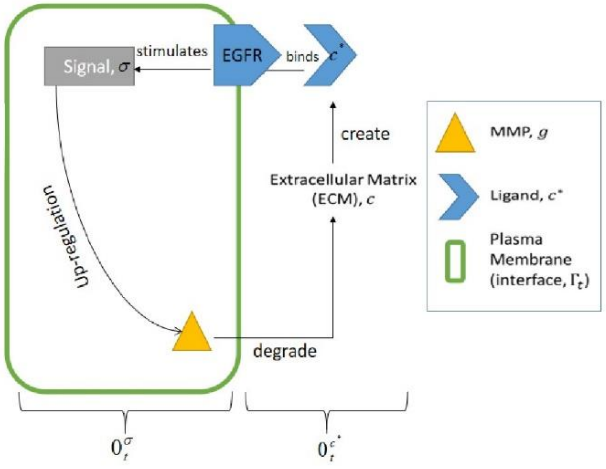

Figure 2 The molecular interaction

Further, the signal transduction stimulates the activity of the actin polymerization. The polymerization process by the actin creates the force that led the interface to the invasion front. Hence, the gradient of the inner signal is applied for the interface velocity. Meanwhile, the partial differential equations method is performed for the velocity extension to gain the information of the velocity from every area of the interface. Since the level set method is implemented, both velocities on the interface and the whole domain are important.

From the above explanations, the equations for the invadopodia formation are stated below.

1. Ligand accumulation, c^*

$$\begin{aligned} \partial_t c^* &= d_{c^*}\Delta c^*, \quad \boldsymbol{x} \in 0_t^{c^*}, \ t \in (0,T], \\ c^*(\boldsymbol{x},0) &= 0, \qquad \boldsymbol{x} \in 0_t^{c^*}, \\ c^*(\boldsymbol{x},t) &= 0, \qquad \boldsymbol{x} \in 0_t^{\sigma}, \ t \in (0,T), \\ c^*|_{\partial\Omega} &= 0, \qquad t \in [0,T], \\ c^*|_{\Gamma_t} &= g|_{\Gamma_t}, \qquad t \in [0,T]. \end{aligned} \tag{1}$$

where d_{c^*} is the ligand diffusivity coefficient.

2. Signal stimulation, σ

$$\begin{aligned} \partial_t \sigma &= d_\sigma \Delta\sigma, \quad \boldsymbol{x} \in 0_t^{\sigma}, \ t \in (0,T], \\ \sigma(\boldsymbol{x},0) &= 0, \qquad \boldsymbol{x} \in 0_t^{\sigma}, \\ \sigma(\boldsymbol{x},t) &= 0, \qquad \boldsymbol{x} \in 0_t^{c^*}, \ t \in (0,T), \\ \sigma|_{\Gamma_t} &= c^*|_{\Gamma_t}, \quad t \in [0,T]. \end{aligned} \tag{2}$$

where d_σ is the signal diffusivity coefficient.

3. Interface velocity, v

$$\boldsymbol{v} = \nabla\sigma, \ t \in (0,T), \tag{3}$$

4. Velocity extension, w

$$(\nabla\psi \cdot \nabla)\boldsymbol{w} = 0, \text{ in } \Omega \tag{4}$$

5. Update the level set

$$\partial_t \psi + \boldsymbol{v} \cdot \nabla\psi = 0, \quad t \in (0,T). \tag{5}$$

2.2 Numerical Methods

In this section, the numerical methods to solve the equations above are presented. First, the explanation of the level set method mostly on tracking the position of interface and consequently determining the position for ligand and signal transduction has been discussed. Next, the finite difference and ghost fluid scheme are described to discuss the procedure to deal with the availability points.

2.2.1 Level Set

In the numerical computation, the first level set is described using $\psi(\boldsymbol{x},0)$ where this symbol is set as a circle equation with radius r (see Equation (6)). The circle-shaped is denoted the plasma membrane of the individual invasive cancer cell. The formation of the invadopodia is the consequence of the motion of the interface. Therefore, the zero-level set function is specified for the interface to detect its motion (refer to Equation (7)). In the meantime, the level set method is implemented to determine the regions of intracellular

and extracellular. The intracellular region where the signal transduction is spotted is defined as the $\psi_{i,j}^t < 0$. On the other hand, for the condition of positive level set $\psi_{i,j}^t > 0$ is used to locate the extracellular region where the ligand is accumulated.

$$\psi_{i,j}^0 = x_i^2 + y_j^2 - r^2, \tag{6}$$

$$\Gamma_t = \{\boldsymbol{x} \in \Omega | \psi_{i,j}^t = 0\}, t \in (0, T) \tag{7}$$

2.2.2 Finite Difference and Ghost Fluid

After the regions for intracellular, extracellular and interface have been determined, the second part that is challenging is the method to solve for the points involved. There are two types of points that have to be emphasized which are regular and neighboring points. The point that is distant from the interface is called regular. Apart from that, the point that is very near to the interface is called the neighboring point. The neighboring points are also determined if their adjacent point is separated by an interface.

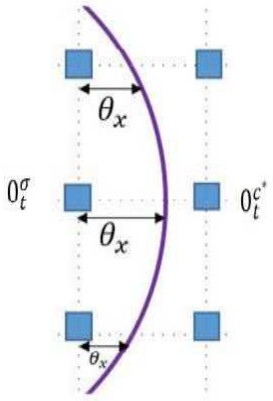

Figure 3 Neighboring points

The second-order centered finite difference approach is suited for the regular points because, in the finite difference approximation, the five-point stencil is on the same region. Nevertheless, it is not preferable to discretize the neighboring point since, from the five-point involved, one of them is separated by the interface. The description of the neighboring points is depicted in Figure 3. From this figure, the region for ligand and signal transduction are separated by the interface. Focused on the signal position, the point on the ligand position is labeled as the ghost value. Here, the ghost fluid method with linear extrapolation is selected. The scheme for the ghost fluid method depending on the four directions has been described in [25]. Hence, Equation (8) is the scheme of the ghost fluid method specifically for the x-derivative in signal transduction position.

$$(u_{xx})_{i,j}^{n+1} = \frac{2}{(1+\theta_x)h^2} u_{i-1,j}^{n+1} - \frac{2}{\theta_x h^2} u_{i,j}^{n+1} + \frac{2}{\theta_x(1+\theta_x)h^2} u_{\Gamma}^{n+1} \tag{8}$$

The θ_x in Equation (8) denoted the distance of the point x_i to the interface. Hence, θ_x is computed using the formula in Equation (9).

$$\theta_x \begin{cases} \dfrac{\psi_i}{\psi_i - \psi_{i-1}}, & if \quad x_\Gamma \in [x_{i-1}, x_i], \\ \dfrac{-\psi_i}{\psi_{i+1} - \psi_i}, & if \quad x_\Gamma \in [x_i, x_{i+1}]. \end{cases} \tag{9}$$

3.0 RESULTS AND DISCUSSION

In this section, the results and discussion are explained in two subsections. First, the formation of invadopodia through the existence of protrusions on the interface is presented. In the next part, the convergence results for the variable involved namely, level set, ligand, and signal transduction are described. For simplicity purpose, the ligand and signal diffusivity coefficients in Section 2.1 are set equal to one.

3.1 The Invadopodium Formation

Figure 4 depicted the formation of invadopodia that has been observed at $t = 1$ (510 iterations). Figure 4(a) displayed the accumulation of ligand in the extracellular region, and it is more clearly spotted at the area of the interface. Because of the ligand and membrane receptor binding, the stimulation of the signal transduction occurred and thus diffused to the intracellular region as illustrated in Figure 4(b). From these two figures, the higher concentration of ligand and signal transduction are observed on the interface due to the MMPs have been concentrated. Consequently, the existence of outward protrusion is spotted at the top of the interface as illustrated in Figure 4(c). This occurrence is due to the interaction inside and outside of a cell and consequently, moved the interface. Here, the invadopodium has been formed to open the passage for the cancer cell to invade the other part of the body.

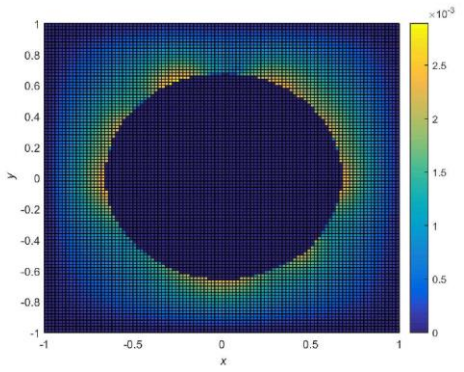

(a)

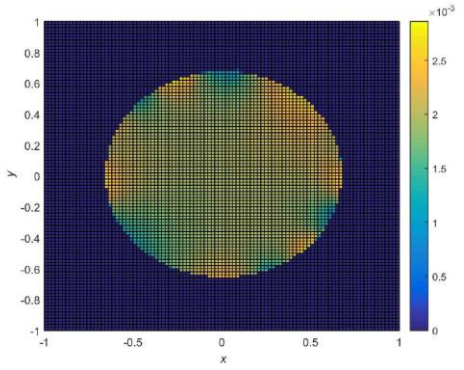

(b)

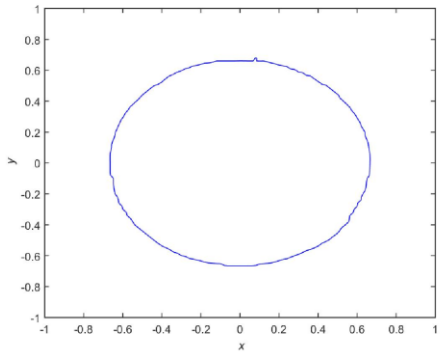

(c)

Figure 4 The formation of invadopodium. (a) Accumulation of ligand; (b) Stimulation of signal transduction; (c) Protrusion

3.2 The Convergence Results

To compute the convergence results, the general shape of protrusions as shown in Figure 4c is taken as the plot of the reference solutions for ψ. Hence, the shape of the protrusions is used as an illustration to end the simulation. The convergence results are provided in Table 1 and Figure 5. The maximum norm for the ψ, c^*, and σ has been observed which has been compared at two different values of space steps, h.

Two different space steps are selected to observe the effect of the grid size with the numerical convergence through the simulation on the variables involved. The results obtained are relatively in good agreement. Based on the simulation, the lower grid size, resulting in a lower error. It is also noticed that significant differences in signal transduction error can be observed when using a smaller grid size.

Table 1 Maximum norm behavior with the grid size reduction

h	It	Errors		
		ψ	c^*	σ
0.2	23	1.132×10^{-4}	3.198×10^{-7}	2.477×10^{-5}
0.04	54	1.059×10^{-4}	2.973×10^{-7}	5.548×10^{-7}

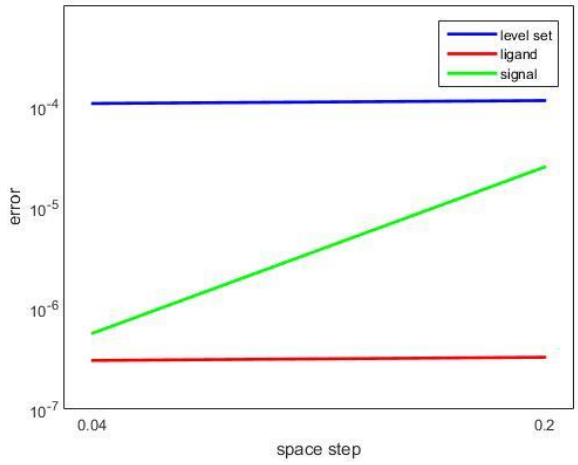

Figure 5 Convergence curve

The convergence profiles for the ψ, c^*, and σ at two different values of space step are depicted in Table 2 and Figure 6. Here, the numerical errors are examined with the increase of iterations. Figure 6(a) illustrates the variation of error for ψ at two different space steps. This figure shows that the error at $h = 0.2$ is higher compared to $h = 0.1$. These findings coincide with the idea that the smaller the grid size, the less error can be achieved. Meanwhile, Figure 6(b) and Figure 6(c) show the errors for ligand and signal transduction. From these two figures, a slight difference in errors for ligand and signal transduction is noticed. Nevertheless, the error show decreases as iteration increased.

Table 2 Numerical errors with the increment of iterations (At $t = 1$)

h	It	Errors		
		ψ	c^*	σ
0.2	1	4.638×10^{-4}	1.149×10^{-3}	1.881×10^{-3}
	50	1.162×10^{-4}	2.874×10^{-7}	9.191×10^{-7}
	100	1.112×10^{-4}	2.683×10^{-7}	1.137×10^{-7}
0.1	1	4.812×10^{-4}	2.732×10^{-3}	2.101×10^{-3}
	50	9.618×10^{-5}	4.917×10^{-7}	9.337×10^{-7}
	100	9.327×10^{-5}	4.398×10^{-7}	1.279×10^{-7}

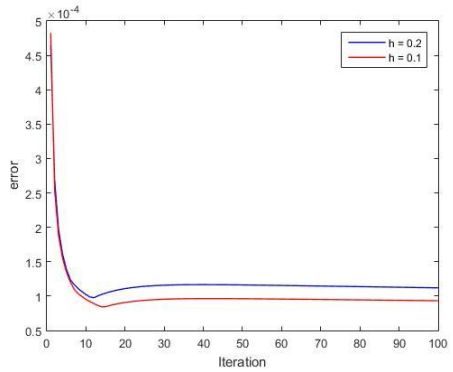

(a)

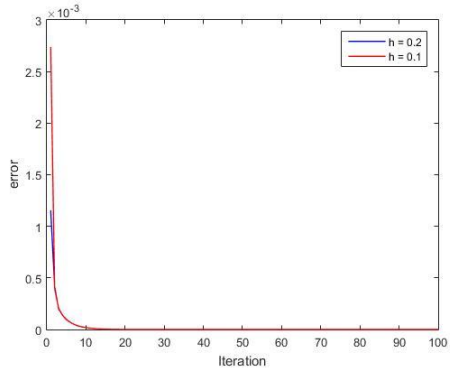

(b)

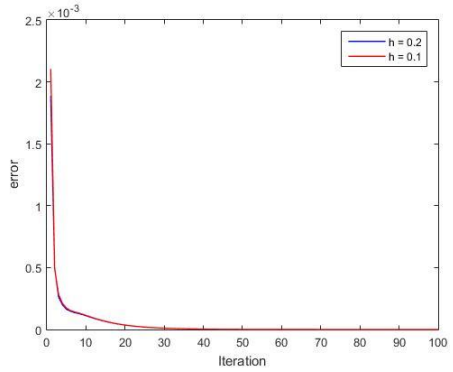

(c)

Figure 6 The convergence profiles. (a) Level set; (b) Ligand; (c) Signal Transduction

4.0 CONCLUSION

This paper investigated the invadopodia formation from the existence of protrusions on the interface. The protrusions formed are the consequence of the physical force created from the polymerization of actin. In this paper, the mathematical modeling is taken as the heat equation to represent the diffusion of ligand and signal transduction to the extracellular and intracellular regions, respectively. The MMPs concentration is assumed as the function g and this is said as the starting point for the formation of invadopodia. Furthermore, the velocity of the interface from the polymerization of actin activity finally moved the interface.

The zero-level set function is used to detect the position of the interface. Furthermore, the intracellular and extracellular regions can be differentiated using the different signs of level set function. On the other hand, the second-order centered finite difference and ghost fluid with linear extrapolation methods are applied for the regular and neighboring points, respectively. Thus, with the aid of the above-mentioned methods, the formation of actin-rich protrusions from the movement of the free boundary interface has been observed.

In the meantime, the distributions of ligand and signal transduction have been obtained to perceive the activity in the extracellular and intracellular regions. Furthermore, the convergence results for the level set, ligand, and signal transduction are observed in the maximum norm approach.

Results showed that the invadopodia are formed due to the activities on the intracellular and extracellular regions. Also, the convergence results gave good outcomes since the error is observed to be smaller as the grid size is decreased. In the future, the equations for MMPs, actin, and membrane receptor should be included in the mathematical modeling due to their important role in the invadopodia formation.

Acknowledgement

This research is fully supported by FRGS grant, FRGS/1/2018/STG06/UTM/02/1. The authors fully acknowledged Kementerian Pendidikan Tinggi Malaysia for the scholarship under the MybrainSC scheme which makes this important research viable and effective.

References

[1] Parekh, A., Ruppender, N. S., Branch, K. M. Sewell-Loftin, M. K., Lin, J., Boyer, P. D. *et al*. 2011. Sensing and Modulation of Invadopodia Across a Wide Range of Rigidities. *Biophys. J*. 100(3): 573-82.
DOI: http://dx.doi.org/10.1016/j.bpj.2010.12.3733.

[2] Parekh, A. and Weaver, A.M. 2016. Regulation of Invadopodia by Mechanical Signaling. *Exp. Cell Res.* 343(1): 89-95.
DOI: https://doi.org/10.1016/j.yexcr.2015.10.038.

[3] Sibony-Benyamini, H. and Gil-Henn, H. 2012. Invadopodia: the Leading Force. *Eur. J. Cell Biol.* 91(11-12): 896-901.
DOI: https://doi.org/10.1016/j.ejcb.2012.04.001.

[4] Enderling, H., Alexander, N., Clark, E., Branch, K., Estrada, L., Crooke, C. *et al*. 2008. Dependence of Invadopodia Function on Collagen Fiber Spacing and Cross-Linking: Computational Modeling and Experimental Evidence. *Biophys. J*. 95: 2203-18.
DOI: https://doi.org/10.1529/biophysj.108.133199.

[5] Eckert, M. A., Lwin, T. M., Chang, A. T., Kim, J., Danis, E., Ohno-Machado, L. *et al*. 2011. Twist1-Induced Invadopodia Formation Promotes Tumor Metastasis. *Cancer Cell*. 19(3): 372-86.
DOI: http://dx.doi.org/10.1016/j.ccr.2011.01.036.

[6] Yamaguchi, H. 2012. Pathological Roles of Invadopodia in Cancer Invasion and Metastasis. *Eur. J. Cell Biol.* 91: 902-7.

DOI: https://doi.org/10.1016/j.ejcb.2012.04.005.
[7] Eddy, R., Weidmann, M., Sharma, V., Condeelis, J. 2017. Tumor Cell Invadopodia: Invasive Protrusions that Orchestrate Metastasis. *Trends Cell Biol.* 27. DOI:https://doi.org/10.1016/j.tcb.2017.03.003.
[8] Saitou, T., Rouzimaimaiti, M., Koshikawa, N., Seiki, M., Ichikawa, K., Suzuki, T. 2012. Mathematical Modeling of Invadopodia Formation. *J. Theor. Biol.* 298:138-46. DOI:https://doi.org/10.1016/j.jtbi.2011.12.018.
[9] Admon, M. A. 2015. Mathematical Modeling and Simulation in an Individual Cancer Cell Associated with Invadopodia Formation. PhD Thesis. Osaka University.
[10] Admon, M. A. and Suzuki, T. 2017. Signal Transduction in the Invadopodia Formation using Fixed Domain Method. *J. Phys. Conf. Ser.* 890: 12036. DOI: http://dx.doi.org/10.1088/1742-6596/890/1/012036.
[11] Noor Azhuan, N. A., Poignard, C., Suzuki, T., Shafie, S., and Admon, M. A. 2019. Two-dimensional Signal Transduction during the Formation of Invadopodia. *MALAYSIAN J. Math. Sci.* 13(2): 155-64.
[12] Gallinato, O., Ohta, M., Poignard, C., and Suzuki, T. 2017. Free Boundary Problem for Cell Protrusion Formations: Theoretical and Numerical Aspects. *J. Math. Biol*. 75(2): 263-307. DOI: https://doi.org/10.1007/s00285-016-1080-7.
[13] Yaacob, N., Noor Azhuan, N. A., Shafie, S., and Admon, M. A. 2019. Numerical Computation of Signal Stimulation from Ligand-EGFR Binding during Invadopodia Formation. *Matematika.* 35(4): 139-48. DOI: https://doi.org/10.11113/matematika.v35.n4.1268.
[14] Strychalski, W., Adalsteinsson, D., and Elston, T. 2010. Simulating Biochemical Signaling Networks in Complex Moving Geometries. *SIAM J. Sci. Comput*. 32(5): 3039-70. DOI: https://doi.org/10.1137/090779693.
[15] Shaikh, J., Bhardwaj, R., and Sharma, A. 2015. A Ghost Fluid Method Based Sharp Interface Level Set Method for Evaporating Droplet. *Procedia IUTAM*. 15: 124-31. DOI: https://doi.org/10.1016/j.piutam.2015.04.018.
[16] Osher, S., and Sethian, J. A. 1988. Fronts Propagating with Curvature-dependent Speed: Algorithms based on Hamilton-Jacobi Formulations. *J. Comput. Phys.* 79(1): 12-49. DOI: https://doi.org/10.1016/0021-9991(88)90002-2.
[17] Sethian, J. A. and Adalsteinsson, D. 1999. The Fast Construction of Extension Velocities in Level Set Methods. *J. Comput. Phys*. 148: 2-22. DOI: https://doi.org/10.1006/jcph.1998.6090.
[18] Chen, S., Merriman, B., Osher, S., and Smereka, P. 1997. A Simple Level Set Method for Solving Stefan Problems. *J Comput. Phys*. 135(1): 8-29. DOI: https://doi.org/10.1006/jcph.1997.5721.
[19] Tan, L. and Zabaras, N. 2007. A Level Set Simulation of Dendritic Solidification of Multi-component Alloys. *J. Comput. Phys.* 221(1): 9-40. DOI: https://doi.org/10.1016/j.jcp.2006.06.003.
[20] Tan, L. and Zabaras, N. 2006. A Level Set Simulation of Dendritic Solidification with Combined Features of Front-tracking and Fixed-domain Methods. *J. Comput. Phys.* 211(1): 36-63 DOI: http://dx.doi.org/10.1016/j.jcp.2005.05.013.
[21] Tan, L. and Zabaras, N. 2007. Modeling the Growth and Interaction of Multiple Dendrites in Solidification using a Level Set Method. *J. Comput. Phys.* 226(1): 131-55. DOI: https://doi.org/10.1016/j.jcp.2007.03.023.
[22] Wilder, J. W., Clemons, C., Golovaty, D., Kreider, K. L., Young, G. W., and Lillard R. S. 2015. An Adaptive Level Set Approach for Modeling Damage Due to Galvanic Corrosion. *J. Eng. Math.* 91(1): 121-42. DOI: http://dx.doi.org/10.1007/s10665-014-9732-3.
[23] Bajger, P., Ashbourn, J. M. A., Manhas, V., Guyot, Y., Lietaert, K., and Geris, L. 2017. Mathematical Modelling of the Degradation Behaviour of Biodegradable Metals. *Biomech. Model Mechanobiol.* 16(1): 227-38. DOI: https://doi.org/10.1007/s10237-016-0812-3.
[24] Guyot, Y., Papantoniou, I., Chai, Y. C., Van Bael, S., Schrooten, J., and Geris, L. 2014. A Computational Model for Cell/ECM Growth on 3D Surfaces using the Level Set Method: A Bone Tissue Engineering Case Study. *Biomech. Model Mechanobiol.* 13(6): 1361-71. DOI: https://doi.org/10.1007/s10237-014-0577-5.
[25] Yaacob, N., Shafie, S., Suzuki, T., and Admon, M. A. 2021. Level Set Method for Free Boundary of Invasive Cancer Cell using Different Functions of Matrix Metalloproteinases. *J. Phys. Conf. Ser.* 1988(1): 012020. DOI:http://dx.doi.org/10.1088/1742-6596/1988/1/012020.